Volume 22, issue 11, November 2007

ISSN 0883-2927

Applied Geochemistry

JOURNAL OF THE INTERNATIONAL ASSOCIATION OF GEOCHEMISTRY

Executive Editor
Associate Editors

*Continued on outside back cover*

See APPLIED GEOCHEMISTRY
on the World Wide Web
http://www.elsevier.com/locate/apgeochem

Available online at www.sciencedirect.com
ScienceDirect
Applied Geochemistry 22 (2007) 2406–2421
Applied Geochemistry
www.elsevier.com/locate/apgeochem

# A sequential extraction to determine the distribution of apatite in granitoid soil mineral pools with application to weathering at the Hubbard Brook Experimental Forest, NH, USA

Carmen A. Nezat [a,*], Joel D. Blum [a], Ruth D. Yanai [b], Steven P. Hamburg [c]

[a] *Department of Geological Sciences, University of Michigan, 1100 North University Avenue, Ann Arbor, MI 48109-1005, USA*
[b] *College of Environmental Science and Forestry, State University of New York, One Forestry Drive, Syracuse, NY 13210-2788, USA*
[c] *Center for Environmental Studies, Box 1943, Brown University, Providence, RI 02912, USA*

Received 16 November 2006; accepted 9 June 2007
Editorial handling by G. Filippelli
Available online 28 June 2007

## Abstract

Mineral weathering in soils is an important source of many nutrients to forest ecosystems. Apatite, a Ca phosphate mineral, occurs in trace amounts in virtually all igneous and metamorphic rocks and is often found as small mineral inclusions in more weathering-resistant silicate minerals. To better understand the distribution of apatite in soils and its exposure to soil solutions, a sequential extraction method was developed to selectively dissolve minerals from soils so that the amount of apatite in contact with soil solutions versus that armored by silicate minerals could be quantified. The use of three molarities of $HNO_3$ (0.01, 0.1 and 1 M) at three temperatures (0, 10, or 20 °C) was explored and it was found that apatite congruently dissolved in 1 M $HNO_3$ at all three temperatures, but did not completely dissolve in weaker $HNO_3$ solutions. Soil horizons, glacial till (i.e., soil parent material), and individual minerals separated from till collected from the Hubbard Brook Experimental Forest (HBEF), NH, were subjected to a 4-step sequential extraction. Chemical analyses of the extracts indicate that 1 M $NH_4Cl$ (pH 7; 20 °C) removes exchangeable ions, 1 M $HNO_3$ at 20 °C primarily dissolves apatite in contact with solutions, 1 M $HNO_3$ at 200 °C primarily dissolves biotite and chlorite (and apatite armored by them), and a mixture of concentrated $HNO_3$, HCl, and HF at 200 °C dissolves the more refractory minerals including muscovite, alkali feldspar, plagioclase feldspar and quartz (and apatite armored by these minerals). This extraction method was applied to soil profiles from HBEF to demonstrate that it could be used to interpret the abundance of apatite and other minerals as a function of depth. Approximately 70% of the apatite in the HBEF soil parent material is exposed to soil solutions; the remaining 30% is armored in more weathering-resistant micas and feldspars. In the upper soil horizons, the only apatite that has not been weathered from the soil occurs as inclusions in micas and feldspars and thus the rate of dissolution of apatite in weathered soil horizons is controlled by silicate mineral dissolution.

---

[*] Corresponding author. Address: Department of Geology, Eastern Washington University, 130 Science Building, Cheney, WA 99004-2439, USA. Tel.: +1 509 359 2286; fax: +1 509 359 4386.
*E-mail address:* carmen.nezat@mail.ewu.edu (C.A. Nezat).

0883-2927/$ - see front matter © 2007 Elsevier Ltd. All rights reserved.
doi:10.1016/j.apgeochem.2007.06.012

## 1. Introduction

Apatite, $Ca_5(PO_4)_3(F,Cl,OH)$, is an accessory mineral that is ubiquitous in igneous and metamorphic (i.e., crystalline) rocks, although it is generally present in low abundance (<1 wt%) as small inclusions in larger silicate minerals. The dissolution rate of apatite is several orders of magnitude faster than most silicate minerals (Guidry and Mackenzie, 2003; Köhler et al., 2005; Valsami-Jones et al., 1998), and consequently its preferential dissolution may strongly influence the surface and groundwater chemistry of watersheds dominated by silicate minerals (Aubert et al., 2001; Hannigan and Sholkovitz, 2001; Oliva et al., 2004). In soils developed on crystalline rocks, apatite is the dominant P-bearing primary mineral. Because P is an essential and sometimes limiting nutrient for plants, apatite dissolution can be an important P source to plants (Chapin III et al., 1994; Crews et al., 1995; Newman, 1995; Schlesinger et al., 1998; Tanner et al., 1998; Vitousek and Farrington, 1997) and may also be a significant source of bioavailable Ca in Ca-poor soils despite its relatively low abundance (Blum et al., 2002; Nezat et al., 2004; Yanai et al., 2005). Uranium-He dating of apatite sampled from soils and eroded alluvium has also recently been used to constrain erosion rates, increasing interest in the susceptibility of apatite to weathering in soil environments (Reiners et al., 2007; Stock et al., 2006).

Apatite can be identified in petrographic thin sections of rocks by its optical properties or its chemical composition (e.g., by energy dispersive X-ray analysis), but its trace occurrence makes it difficult to quantify its abundance in rocks or soils using these methods. The total Ca and P in a bulk soil digest are insufficient to estimate the amount of apatite in soil because these elements are not exclusively found in apatite. For example, soil organic matter and secondary Fe and Al oxides can contain significant amounts of P, and silicate minerals contain most of the Ca in soils derived from crystalline silicate parent material. The inclusion of apatite within unfractured silicate minerals presents another complication; inclusions are not exposed to soil solutions until the host minerals are dissolved, and thus apatite armored within weathering-resistant silicate minerals may persist in soils. Therefore, the total apatite content of rocks and soils may overestimate the amount of apatite exposed to soil solution.

Extraction methods exist to apportion P from sediments and soils into pools of differing availability, such as exchangeable, carbonate-bound, Al and Fe oxide-bound, organically bound, and primary apatite (Hedley et al., 1982; Leleyter and Probst, 1999; Ruttenberg, 1992; Tessler et al., 1979; Williams et al., 1980). However, some of the extracting solutions contain Na and Mg, elements that are important to quantify in weathering studies. In addition, some soil extraction procedures may dissolve apatite during more than one step and are thus not adequately selective (Aubert et al., 2004; Leleyter and Probst, 1999). Those methods that do selectively dissolve apatite use HCl (Ruttenberg, 1992; Williams et al., 1980), which forms chloride molecular interferences that can be problematic for analysis by inductively-coupled plasma mass spectrometry.

In previous investigations (Blum et al., 2002; Hamburg et al., 2003), a sequential extraction procedure was applied to soils containing Ca-bearing minerals to examine the relative availability of Ca pools. The 4 extracting solutions were: 1 M $NH_4Cl$ at room temperature, 1 M $HNO_3$ at room temperature, concentrated $HNO_3$ at 200 °C, and a solution of concentrated HF, HCl and $HNO_3$ at 200 °C. Based on the chemical composition of the extracts, it was inferred that the 4 steps of the procedure dissolved Ca predominantly associated with the soil exchange pool, Ca in apatite, Ca in easily-weathered silicates and Ca in more weathering-resistant silicate minerals, respectively. In this paper, the extraction procedure was systematically evaluated and the full major element chemistry of the soil minerals and extraction solutions explored. First, this procedure was applied to individual minerals separated from a granitoid glacial till (i.e., soil parent material) collected at the Hubbard Book Experimental Forest (HBEF, New Hampshire, USA) to identify mineral compositions and to determine which minerals were dissolved during each step. Next, the influence of acid strength and temperature on the isolation of apatite in the second extraction step was identified. Finally, to quantify the amount of elements associated with organic matter, secondary minerals and primary minerals in soils, this method was applied to soils from HBEF where the weathering of primary silicate minerals and accumulation of secondary minerals in soil profiles has previously been characterized (Johnson et al., 1991; Nezat et al., 2004).

## 2. Methods

### 2.1. Soil sample collection

Soil and soil parent material (glacial till) were collected from Watershed 1 (W-1) of the HBEF in the White Mountains of central New Hampshire (43 °57′N, 71°44′W). The soils are relatively thin (mean thickness of 50 cm) and moderately well-drained Spodosols (Haplorthods) developed in basal till deposited by continental ice sheets that receded from the area ~14 ka ago (Davis et al., 1985; Likens et al., 1977). The till is derived largely from local bedrock: Silurian-aged Rangeley Formation, a pelitic schist and meta-sandstone, and Devonian Kinsman granodiorite, a foliated granitoid rock with megacrysts of K feldspar (Barton et al., 1997). The vegetation of HBEF is characteristic of the northern hardwood forest (Bormann and Likens, 1979).

One large sample of deep and unweathered soil parent material was collected for mineral separation from a trench that had been previously excavated by backhoe just outside the boundary of the lower part of W-1. A vertical face was cleared to create a fresh surface and material was collected from a depth of 160 cm below the surface, ~90 cm below the top of the C horizon.

Forty-five locations within W-1 were randomly selected for soil sampling during the summer of 1997 (Nezat et al., 2004). Soil was quantitatively excavated below a 0.7 m by 0.7 m frame to an average depth of ~70 cm. Samples were collected from 6 horizons (Oa, E, Bh, Bs1, Bs2, C), sieved through a 2-mm screen, and oven-dried at 105 °C. To reduce the total number of analyses but retain large-scale spatial patterns, the watershed was divided into six areas which included two areas in each of three elevation zones. Each area contained between four and 11 soil pits. For each horizon in each area, a weighted composite sample was created by combining 1% (by mass) of soil of like horizons from soil pits within that area. This procedure resulted in 36 soil samples (six horizons from each of six areas) for analysis.

### 2.2. Mineral separates

The large sample of soil parent material was crushed and the 100 to 300 μm size fraction was separated (using heavy liquids and a magnetic separator) into five samples highly enriched in one of the following: apatite, K feldspar, plagioclase, muscovite, or biotite. To check the purity of the separates, a subsample of approximately 100 mineral grains from each separate was mounted on C tape and C coated. Minerals were identified using an energy dispersive spectrometer (EDS) on a Hitachi S3200N scanning electron microscope (SEM); the area of mineral grains was calculated from BSE digital images using an image analysis software (Scion Image) to estimate the relative abundance of each mineral. The apatite separate was not checked for purity by SEM/EDS due to limited sample size; its purity was inferred from the chemistry of the digests of the separate.

### 2.3. Sequential extraction procedure

Representative 0.5 g subsamples of soils, glacial till, and mineral separates were sequentially reacted with each of the following ultra-pure solutions: 5 mL of 1 M $NH_4Cl$ (pH 7) in a screw-top polypropylene tube at room temperature (~20 °C) on a shaker table for 20 h; 5 mL of 1 M $HNO_3$ in a screw-top polypropylene tube at room temperature (~20 °C) on a shaker table for 20 h; 5 mL of 1 M $HNO_3$ at 200 °C for 20 min (by microwave at ~20 MPa); and, a solution of 8 mL of concentrated $HNO_3$, 1 mL HCl, and 1 mL HF at 200 °C for 15 min (by microwave at ~20 MPa; this is referred to as the HF solution). The last two steps were performed in reinforced Teflon microwave vessels (CEM MARS 5, XP-1500 vessels, Matthews, NC, USA). After each extraction, the solution was centrifuged and the supernatant was pipetted into a Teflon beaker, evaporated to dryness on a hot plate, redissolved in 1 mL of concentrated $HNO_3$, evaporated again, and redissolved in 10–20 mL of 5% $HNO_3$ for chemical analysis. The mineral residue from each extraction step was carried to the subsequent step.

### 2.4. Isolation of apatite dissolution

To determine the optimal conditions for dissolving apatite while minimizing dissolution of other minerals, nine subsamples of HBEF C horizon soil were used. First, the exchangeable fraction was removed by adding 5 mL of 1 M $NH_4Cl$ solution (pH 7) to 0.5 g of dried C horizon soil and shaking for 20 h at room temperature (~20 °C). Next, each subsample was treated with a different combination of molarity and temperature of extracting solution.

The three molarities were 0.01 M, 0.1 M and 1 M $HNO_3$ (pH of 2, 1 and 0, respectively), and the 3 temperatures were 0, 10 and 20 °C. The 0 and 10 °C extractions were performed in a standard laboratory refrigerator and temperature was monitored using a digital thermometer.

### 2.5. Chemical analysis of extracts

Extracts were analyzed on an inductively coupled plasma-optical emission spectrometer (Optima 3300 DV, Perkin–Elmer, Norwalk, CT, USA) using NIST-traceable standard solutions and 5- to 8-point calibration curves. The elements Al, Ca, Fe, K, Mg, Na, P, Si, Sr and Ti were determined. Silicon is not reported for the final extract because Si is volatilized during extraction with HF. The lack of significant contamination during the sequential extraction was confirmed by multiple analyses of procedural blanks. Analysis of certified reference materials Soil Solution A and River Sediment Solution B (High Purity Standards, Charleston, SC, USA) indicate that the accuracy of the chemical analysis was within ±5%.

To distinguish subtle differences in the relative dissolution of minerals such as apatite and biotite, $^{87}Sr/^{86}Sr$ ratios were measured in the extracts obtained at different temperatures and molarities from C horizon samples (described above) and in the apatite separate. Sample aliquots containing ~100 ng of Sr were eluted through quartz columns with Eichrom Sr-Spec resin. Strontium fractions were loaded with 1 μL of $H_3PO_4$ and $Ta_2O_5$ powder on W filaments. Fifty to 200 $^{87}Sr/^{86}Sr$ ratios were measured for each sample on a multiple-collector thermal ionization mass spectrometer (Finnigan MAT 262, Bremen, Germany) in static mode, yielding internal precisions of at least ±0.000030 ($2\sigma$). The $^{87}Sr/^{86}Sr$ ratios were normalized to an $^{86}Sr/^{88}Sr$ value of 0.1194. Measurements of NBS987 had a mean $^{87}Sr/^{86}Sr$ ratio of $0.710238 \pm 0.000025$ ($2\sigma$, $n = 26$) during the period of analysis.

## 3. Results

### 3.1. Sequential extraction of mineral separates

The density and magnetic separations of minerals from the glacial till parent material yielded separates that varied in purity (Table 1). Separation of minerals was not complete because some minerals have similar physical properties (e.g., alkali feldspar, plagioclase and quartz), are intergrown (e.g., biotite and muscovite), or have mineral inclusions (e.g., apatite included within biotite). The sequential extraction procedure was applied to each mineral separate and to the glacial till from which the minerals were separated (Table 2).

Table 1
Mineral composition of separates determined by scanning electron microscopy and energy dispersive spectrometry

| | (% of each mineral in separate)[a] | | | |
|---|---|---|---|---|
| | Plagioclase separate | Alkali feldspar separate | Muscovite separate | Biotite separate |
| Plagioclase | **55.2** | 17.1 | 5.3 | 6.0 |
| Alkali feldspar | 7.0 | **82.6** | 2.1 | 2.6 |
| Muscovite | 1.1 | ND | **58.3** | 4.7 |
| Biotite | 6.7 | ND | 18.5 | **62.5** |
| Chlorite | ND | ND | 1.8 | 4.6 |
| Quartz | 26.8 | 0.3 | 11.0 | 4.3 |
| Hornblende | ND | ND | 2.3 | 10.8 |
| Other | 3.2 | ND | 0.7 | 4.5 |
| Total | 96.8 | 100.0 | 99.3 | 95.5 |

"Other" minerals include apatite, ilmenite, zircon and epidote.

[a] ND indicates not detected.

Calcium and P were the dominant elements in all extracts of the apatite mineral separate, indicating that the separate was ~98% pure (Table 2, Fig. 1a). The first extract, a 1 M $NH_4Cl$ solution, removed <0.01% of the Ca and P in the bulk sample. The 1 M $HNO_3$ extract at 20 °C and 200 °C removed ~40% and ~60%, respectively, of the total Ca and P in a Ca:P ratio of 5:3 (the stoichiometric ratio in apatite). The only other measured element released in significant quantity was Al, which was removed mainly in the HF solution and accounted for only ~1% of the total of the elements analyzed.

Most of the plagioclase separate was extracted by the HF solution (Table 2, Fig. 1b). The 1 M $NH_4Cl$ extraction step removed only ~0.04% of the total of the elements analyzed. The 1 M $HNO_3$ extract (at 20 °C) removed some Al, Ca, Fe and P, presumably from apatite inclusions and Fe and Al oxides, but these accounted for only ~3% of the total of the elements analyzed (Table 1). The 1 M $HNO_3$ extract of plagioclase (at 200 °C) dissolved Al, Ca, K and Na totaling ~6% of the separate. The HF solution extracted more than 90% of the separate and contained Al, Ca, K and Na. The K is presumably derived from alkali feldspar which constitutes 13% of the total feldspars in the plagioclase separate (Table 2); small amounts of Fe, Mg and P in the

Table 2
Chemical composition of extractions of mineral separates and glacial till

| | Al | Ca | Fe | K | Mg | Na | P | Si | Sr | Ti |
|---|---|---|---|---|---|---|---|---|---|---|
| | μmol/g | | | | | | | | | |
| *1 M $NH_4Cl$ extract* | | | | | | | | | | |
| Apatite | BDL[a] | BDL | BDL | BDL | BDL | BDL | BDL | BDL | BDL | BDL |
| Plagioclase | BDL | 0.9 | 0.173 | 0.121 | 0.512 | BDL | BDL | BDL | BDL | BDL |
| Alkali feldspar | BDL | 0.7 | 0.0130 | 0.109 | 0.380 | BDL | BDL | BDL | BDL | BDL |
| Muscovite | BDL | BDL | BDL | 0.342 | BDL | BDL | BDL | BDL | BDL | BDL |
| Glacial till | BDL | BDL | 0.373 | 0.394 | BDL | BDL | BDL | BDL | BDL | 0.037 |
| *1 M $HNO_3$ extract(at 20 °C)* | | | | | | | | | | |
| Apatite[b] | 40.8 | 3459 | 11.2 | 3.87 | 3.57 | 10.0 | 2190 | 45.1 | 1.31 | 0.469 |
| Plagioclase | 45.4 | 41.5 | 9.77 | 1.28 | 2.57 | BDL | 26.2 | 22.9 | 0.0204 | 0.332 |
| Alkali feldspar | 38.3 | 8.08 | 7.15 | 1.01 | 1.02 | BDL | 6.23 | 16.2 | 0.0026 | 0.170 |
| Muscovite | 113 | 35.3 | 31.8 | 2.57 | 6.94 | BDL | 21.0 | 47.3 | 0.0245 | 0.690 |
| Biotite | 238 | 51.0 | 179 | 1.51 | 31.8 | BDL | 27.3 | 79.2 | 0.0610 | 3.95 |
| Glacial till | 97.0 | 26.0 | 26.8 | 3.10 | 9.43 | BDL | 15.9 | 43.0 | 0.00848 | 0.837 |
| *1 M $HNO_3$ extract (at 200 °C)* | | | | | | | | | | |
| Apatite | 20.3 | 5315 | 3.89 | 4.81 | 0.587 | 14.6 | 3279 | 42.7 | 1.29 | 0.571 |
| Plagioclase | 140 | 37.1 | 26.9 | 11.4 | 14.1 | 36.9 | 4.16 | 109 | 0.161 | 2.44 |
| Alkali feldspar | 56.4 | 1.32 | 13.7 | 19.2 | 5.62 | 15.4 | 2.04 | 52.5 | 0.0204 | 0.625 |
| Muscovite | 353 | 25.6 | 310 | 58.2 | 172 | 12.0 | 2.51 | 115 | 0.0833 | 12.2 |
| Biotite | 1294 | 22.9 | 1583 | 258 | 759 | 15.9 | 13.5 | 414 | 0.0697 | 53.6 |
| Glacial till | 125 | 3.86 | 98.3 | 33.8 | 52.1 | 5.43 | 2.32 | 137 | 0.0121 | 5.94 |
| *HF/HCl/$HNO_3$ extract* | | | | | | | | | | |
| Apatite | 129 | 13.2 | 0.384 | 12.9 | BDL | 18.2 | 17.5 | NR[c] | 0.00899 | 4.46 |
| Plagioclase | 2298 | 531 | 26.5 | 204 | 14.0 | 1204 | 5.33 | NR | 2.85 | 15.3 |
| Alkali feldspar | 3312 | 73.5 | 4.58 | 1928 | 3.01 | 1083 | 7.88 | NR | 1.55 | 1.65 |
| Muscovite | 2164 | 174 | 191 | 830 | 60.4 | 690 | BDL | NR | 1.25 | 63.4 |
| Biotite | 1609 | 231 | 498 | 458 | 213 | 669 | BDL | NR | 1.99 | 169 |
| Glacial till | 1663 | 167 | 104 | 700 | 26.4 | 793 | 4.48 | NR | 0.972 | 27.9 |
| *Sum of extracts* | | | | | | | | | | |
| Apatite | 190 | 8788 | 15.4 | 21.6 | 4.16 | 42.8 | 5486 | NR | 2.62 | 5.52 |
| Plagioclase | 2483 | 610 | 63.4 | 217 | 31.2 | 1241 | 35.7 | NR | 3.03 | 18.1 |
| Alkali feldspar | 3406 | 83.6 | 25.5 | 1948 | 10.0 | 1099 | 16.2 | NR | 1.57 | 2.45 |
| Muscovite | 2630 | 234 | 533 | 892Z | 239 | 702 | 23.6 | NR | 1.36 | 76.2 |
| Biotite | 3141 | 305 | 2260 | 717 | 1004 | 685 | 40.7 | NR | 2.12 | 226 |
| Glacial till | 1884 | 197 | 230 | 737 | 88.0 | 799 | 22.7 | NR | 0.992 | 34.7 |
| *Ideal chemical composition of minerals*[d] | | | | | | | | | | |
| Apatite | – | 9920 | – | – | – | – | 5952 | – | – | – |
| Plagiocalse | 4600 | 657 | – | – | – | 3113 | – | 10,459 | – | – |
| Alkali feldspar | 3597 | – | – | 3597 | – | – | – | 10,791 | – | – |
| Muscovite | 7538 | – | – | 2513 | – | – | – | 7538 | – | – |
| Biotite | 3985 | – | 3454 | 1689 | 1589 | – | – | 6156 | – | 411 |

[a] BDL indicates "below detection limit."

[b] The $^{87}Sr/^{86}Sr$ of the 1 M $HNO_3$ extract of the apatite separate is 0.715281.

[c] NR indicates "not reported." Si concentrations in the HF/HCl/$HNO_3$ extract and the sum of extracts are not reported because Si is volatilized during HF digestion.

[d] The chemical compositions of plagioclase and biotite were measured by microprobe analysis and reported in Nezat et al. (2004). Apatite, alkali feldspar, and muscovite were assumed to have the following compositions: $Ca_5(PO_4)_3$ F, $KAlSi_3O_8$, and $KAl_2(AlSi_3O_{10})(OH)_2$, respectively. Except for Ti in biotite, the concentrations of only major elements were calculated. Dashed lines indicate values not calculated.

HF solution suggest the presence of other minerals possibly as inclusions in the feldspars (Fig. 1b).

Like the plagioclase separate, most of the alkali feldspar separate was extracted by the HF solution (Table 2, Fig. 1c). The 1 M $NH_4Cl$ removed only ~0.2% of the total of the elements analyzed. The 1 M $HNO_3$ (at 20 °C) extracted small amounts of Al, Ca, Fe and P, which accounted for ~1% of

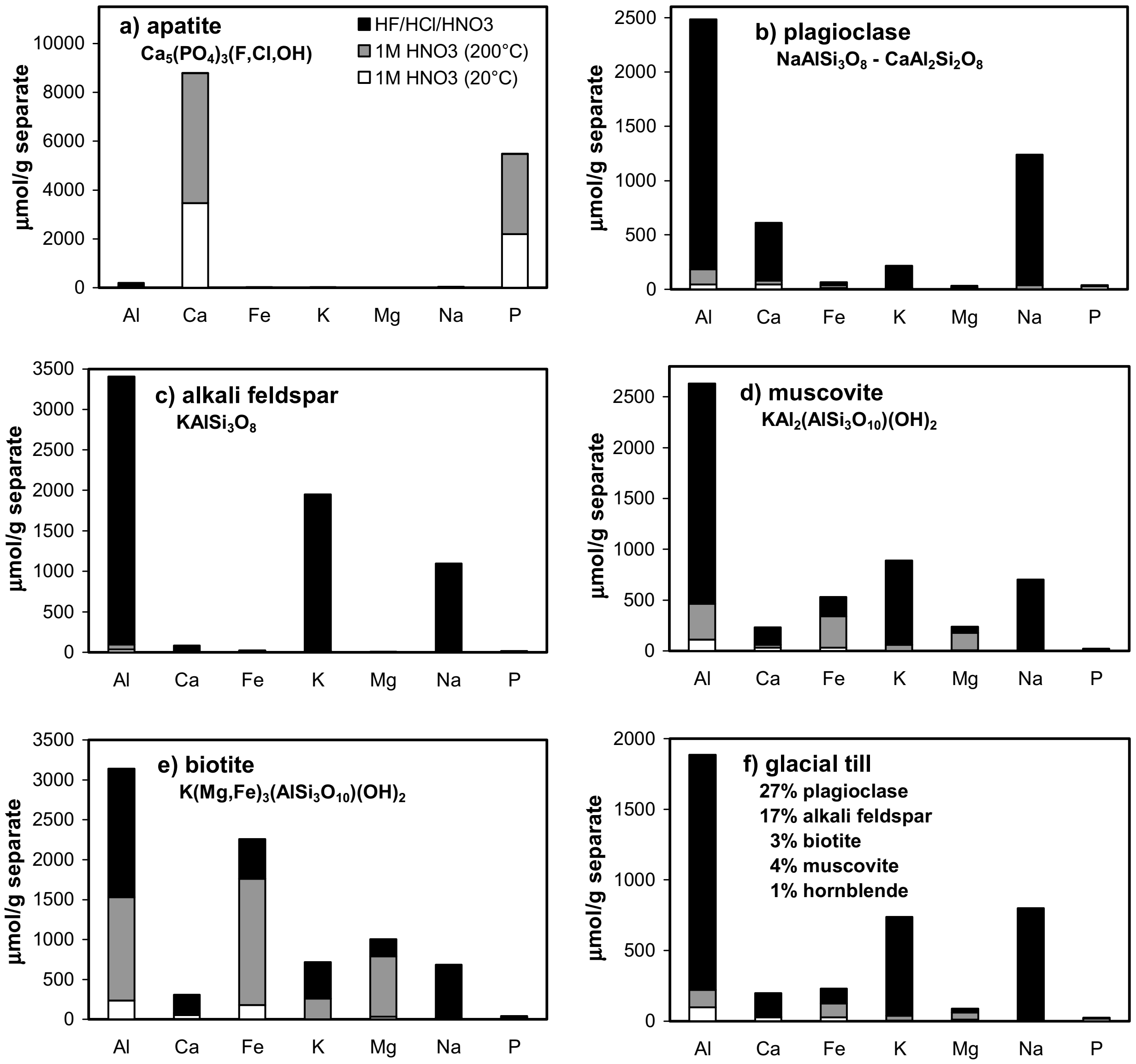

Fig. 1. Chemical composition of sequential extracts of minerals separated from HBEF glacial till. Mineral separates are not pure (Table 1), but are named according to the dominant mineral in the separate. The general formula for each mineral is given. The sequential extract of the bulk glacial till is shown for comparison; the composition of the glacial till is from Nezat et al. (2004). The 1 M $NH_4Cl$ extracts are not included because they are ≪1% of the total, and too small to be seen at this scale.

the total of the elements analyzed, and the 1 M $HNO_3$ (at 200 °C) dissolved some Al, Fe and Mg, which totaled ~2% of the total of the elements analyzed. The HF solution, which extracted 97% of the total of the elements analyzed, contained predominantly Al, Ca, K and Na from the dissolution of alkali feldspar and plagioclase, the latter of which constituted 17% of the alkali feldspar separate.

Most of the muscovite separate was dissolved by the HF solution (Table 2, Fig. 1d). The 1 M $NH_4Cl$ extraction of muscovite removed only ~0.01% of the total of the elements analyzed. As in the extraction of the feldspar separates, the 1 M $HNO_3$ (at 20 °C) extract dissolved Al, Ca, Fe and P, amounting to <4% of the total of the elements analyzed. The 1 M $HNO_3$ extract (at 200 °C) dissolved ~18% of the total of the elements analyzed and had high concentrations of Al, Fe, K and Mg. These elements are in biotite, chlorite, and hornblende, minerals that are present in the muscovite separate as impurities. The HF solution dissolved most of the muscovite separate and contained Al, Ca, Fe, K, Mg, and Na, indicating dissolution of muscovite along with the plagioclase and alkali feldspar that were present as impurities (Table 1).

In contrast to the feldspars and muscovite separates, a significant proportion of the biotite separate was dissolved by the 1 M $HNO_3$ (at 200 °C) extraction (Table 2, Fig. 1e). The 1 M $NH_4Cl$ extraction removed only ~0.01% of the total of the elements analyzed. The 1 M $HNO_3$ (at 20 °C) removed ~6% of the total of the elements analyzed, most of which was Al, Ca, Fe and P (Fig. 1e). The 1 M $HNO_3$ (at 200 °C) and the HF solution extracted roughly equal portions of the total elements analyzed (Table 1). The 1 M $HNO_3$ extract (at 200 °C) contained Al, Fe, K and Mg, elements present in biotite, muscovite, chlorite and hornblende. The HF solution extracted Al, Ca, Fe, K, Mg and Na, indicative of the dissolution of plagioclase, alkali feldspar and muscovite.

### 3.2. Sequential extraction of glacial till

The chemical composition of the bulk glacial till reflects the dissolution of all of the minerals in the mineral separates, combined in their naturally occurring proportions. The 1 M $NH_4Cl$ extracted <0.1% of the total of the elements analyzed. The second step in the sequential extraction method (1 M $HNO_3$ at 20 °C) was intended to target the dissolution of apatite. The 1 M $HNO_3$ (at 20 °C) removed ~10% of the total of the elements analyzed, and was composed mostly of Al, Ca, Fe and P; small amounts of K, Mg and Si were also released (Fig. 1f). The 1 M $HNO_3$ (at 200 °C) extracted ~15%, and the HF solution ~75%, of the total of the elements analyzed in the glacial till samples.

### 3.3. Effect of $HNO_3$ molarity and temperature on apatite dissolution

The extraction of glacial till at 3 $HNO_3$ molarities and 3 temperatures tested the effect of the concentration and temperature of $HNO_3$ on the specificity and congruency of apatite dissolution (Table 3, Fig. 2). At the $HNO_3$ concentration of 0.01 M, apatite did not dissolve appreciably at any of the temperatures investigated (0, 10 or 20 °C). In the 0.1 M $HNO_3$ extract, a considerable amount of Ca was released into solution at all three temperatures, but less P than expected from congruent dissolution of apatite (represented by the dashed line in Fig. 2a). The 1 M $HNO_3$ extract removed the highest concentrations of Ca and P and had a Ca:P ratio identical to that of apatite (5:3), indicating the congruent dissolution of apatite. The $^{87}Sr/^{86}Sr$ ratio of the 0.1 and 1 M extracts (0.716980–0.721517) were similar to that of the HBEF apatite separate (0.715281) and much lower than the $^{87}Sr/^{86}Sr$ ratio of the 0.01 M extracts (>0.743892; Fig. 2b).

Temperature had little effect on the efficacy of apatite dissolution with 1 M $HNO_3$ (Fig. 2a). However, minor amounts of other elements were released into solution in the 1 M $HNO_3$ extracts as temperature increased (Fig. 2c–f). Among the elements that were analyzed, some were strongly correlated with each other: Fe, K, Mg and Ti concentrations were correlated (for each pair $r^2 > 0.9$, $p < 0.1$ at $\alpha = 0.01$ except that $p = 0.11$ between Fe and Mg), and Na and Sr concentrations were correlated ($r^2 = 0.9936$, $p < 0.1$).

### 3.4. Sequential extraction of soil profiles

The sequential extraction procedure was applied to the six composite soil profiles that were derived from 45 soil pits at the HBEF in order to extend the interpretations of the sequential extracts of parent materials to weathered horizons and to demonstrate how this method can be used to provide insight into soil-forming processes.

The 1 M $NH_4Cl$ extract represented a very small fraction (<1%) of the total soil chemical inventory and was dominated by Ca, K and Mg (Fig. 3). The cation concentrations in the 1 M $NH_4Cl$

Table 3
Chemical composition of extracts (performed at various molarities and temperatures) of a C horizon sample

| Temperature (°C) | $HNO_3$ (M) | µmol/g sample | | | | | | | | nmol/g sample | | $^{87}Sr/^{86}Sr$ |
|---|---|---|---|---|---|---|---|---|---|---|---|---|
| | | Al | Ca | Fe | K | Mg | Na | P | Si | Sr | Ti | |
| 20 | 0.01 | 2.75 | 0.0247 | 0.445 | 0.107 | 0.0758 | 0.0233 | 0.0321 | 1.26 | <0.17 | 25.1 | 0.743892 |
| 20 | 0.1 | 77.8 | 15.2 | 0.508 | 0.109 | 0.0822 | 0.132 | 2.46 | 8.25 | 5.04 | 10.3 | 0.719653 |
| 20 | 1 | 172 | 18.1 | 21.4 | 0.499 | 2.57 | 0.338 | 12.0 | 15.5 | 6.85 | 512 | 0.721517 |
| 10 | 0.01 | 3.96 | 0.160 | 0.649 | 0.104 | 0.0973 | 0.0384 | 0.110 | 1.34 | <0.17 | 30.3 | 0.746862 |
| 10 | 0.1 | 80.0 | 13.4 | 0.307 | 0.0925 | 0.0501 | 0.125 | 3.37 | 6.81 | 4.74 | 10.9 | 0.717267 |
| 10 | 1 | 143 | 15.2 | 12.8 | 0.272 | 0.563 | 0.274 | 9.79 | 4.55 | 6.76 | 297 | 0.720752 |
| 0 | 0.01 | 3.51 | 0.134 | 0.571 | 0.0888 | 0.0825 | 0.0237 | 0.116 | 4.57 | <0.17 | 27.8 | 0.752232 |
| 0 | 0.1 | 72.8 | 11.6 | 0.229 | 0.0748 | 0.0476 | 0.0862 | 3.08 | 7.57 | 4.78 | 10.5 | 0.718473 |
| 0 | 1 | 167 | 18.3 | 8.83 | 0.169 | 0.208 | 0.197 | 12.1 | 24.5 | 6.68 | 215 | 0.716980 |

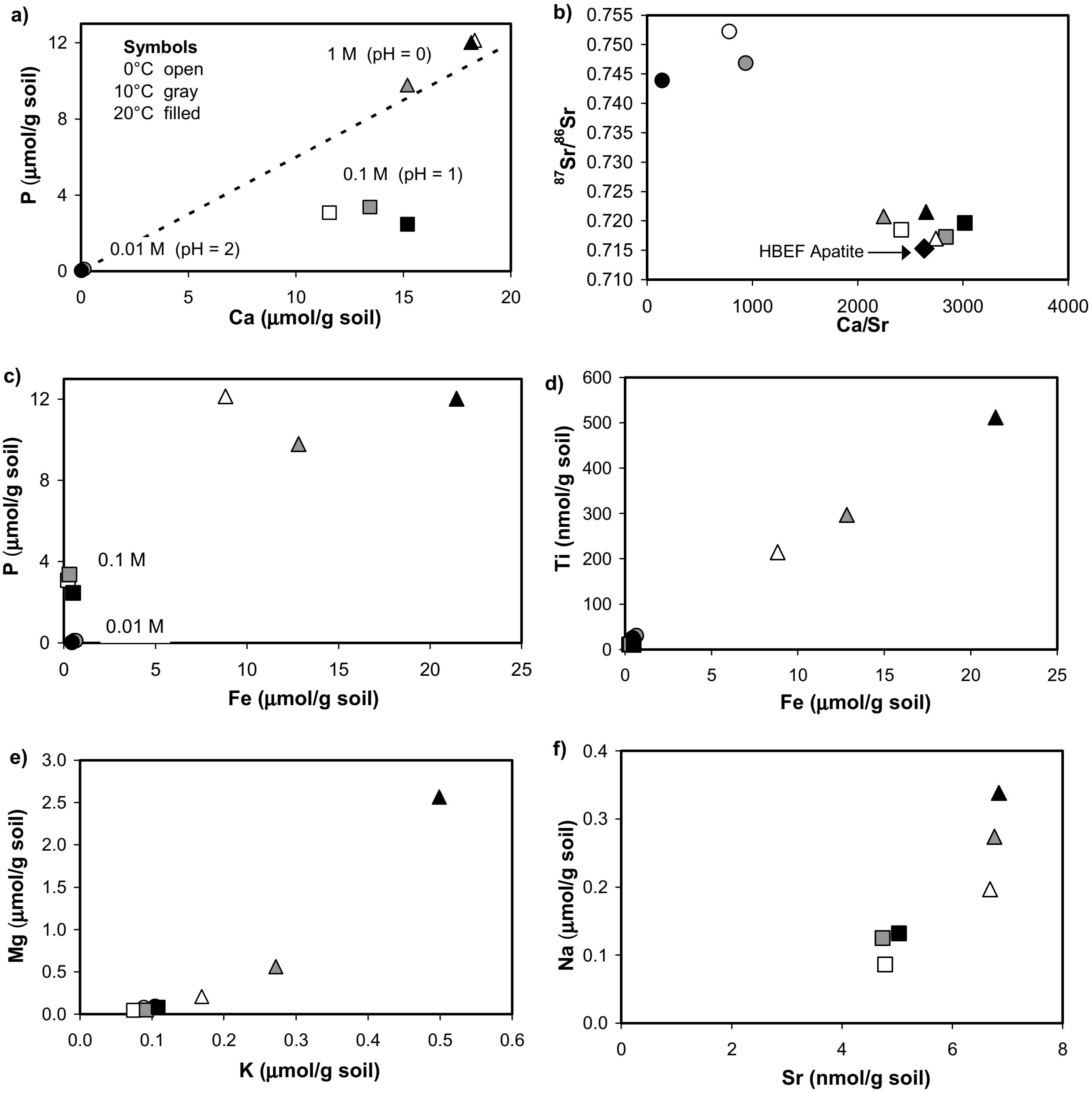

Fig. 2. Chemical composition of C horizon soil extracted by 0.01 M, 0.1 M, or 1 M $HNO_3$ solution at 0, 10 or 20 °C. The pH values of the solutions are 2, 1 and 0, respectively. The 0.01 M, 0.1 M, and1 M $HNO_3$ solutions are represented by circles, squares and triangles, respectively; the extracts at 0, 10 and 20 °C are represented by open, gray and black symbols, respectively. (a) P versus Ca concentrations. The dashed line represents the P:Ca ratio of apatite (0.6). (b) $^{87}Sr/^{86}Sr$ versus Ca/Sr. (c) P versus Fe concentrations. (d) Ti versus Fe concentrations. (e) Mg versus K concentrations. (f) Sr versus Na concentrations. The Sr concentrations were below detection limit (0.17 mmol/g sample) in the 0.01 M extracts.

extracts were highest in the Oa horizon, lowest in the E and C horizons and intermediate in the Bh, Bs1 and Bs2 horizons.

The 1 M $HNO_3$ extract (at 20 °C) was dominated by Fe released from the Bh, Bs1 and Bs2 horizons and Ca and P released from the C horizon (Fig. 3). Potassium, Mg and Na were very low in this extract in all horizons.

A large proportion of the Fe and Mg in the soil was released by the 1 M $HNO_3$ extract (at 200 °C). Large amounts of P were also removed by the 1 M $HNO_3$ extract (at 200 °C) in the organic and B horizons. In contrast, Ca, Na and K concentrations in this extract represent only a small fraction of the total soil pools (Fig. 3). The composition of this extract showed little variation with depth.

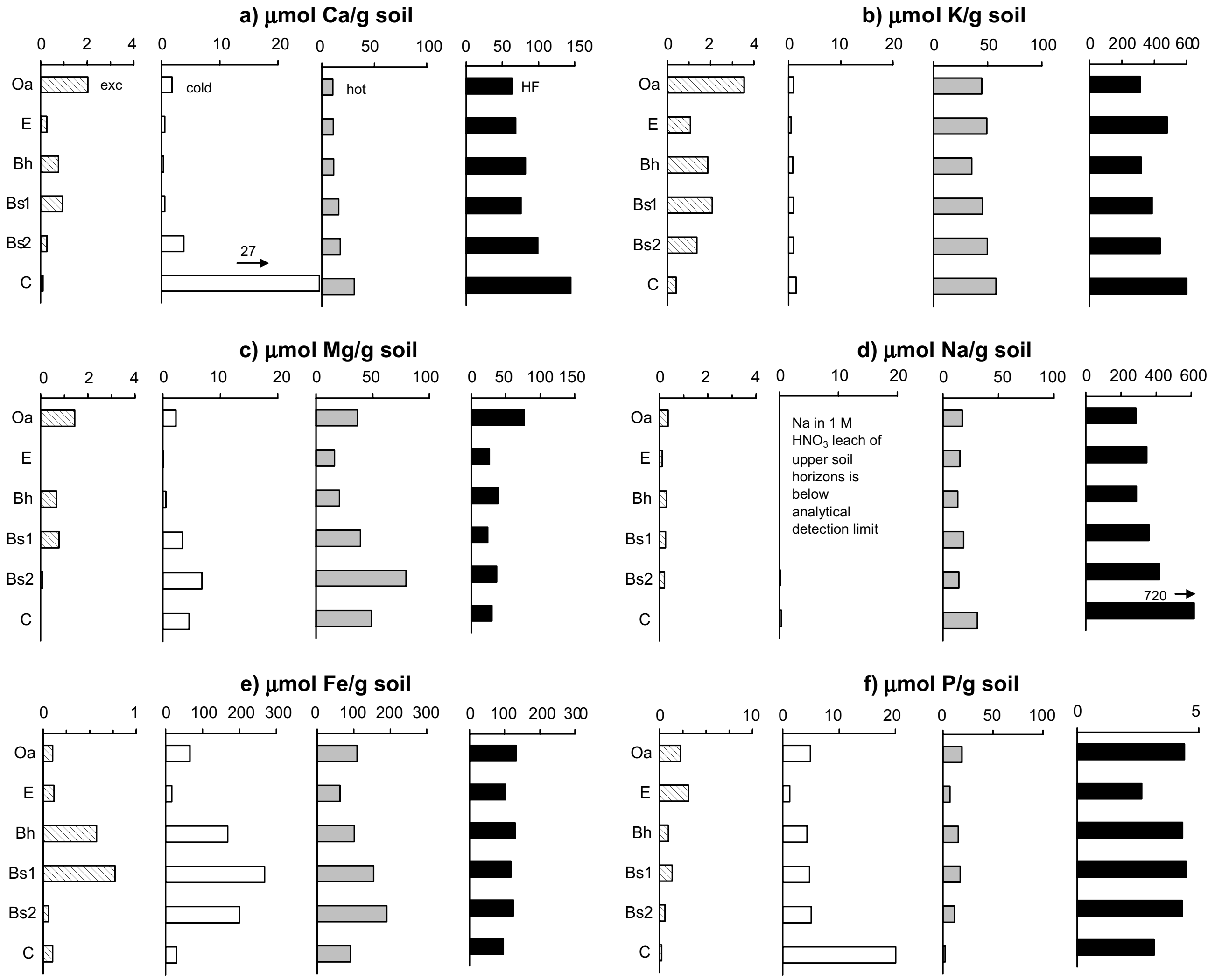

Fig. 3. Distribution of elements with depth in a composite soil profile from the Hubbard Brook Experimental Forest. The chemical composition of this composite profile is represented by black symbols in Fig. 4 and enlarged symbols in Figs. 5 and 6.

The HF/HCl/$HNO_3$ solution extracted most of the Ca, K and Na in each soil horizon (Fig. 3). Magnesium and Fe were released in amounts approximately equal to the 1 M $HNO_3$ extract (at 200 °C), and P concentrations were relatively low in this extract. This extract also showed little variation in composition with depth, with the exception that Ca and Na were higher in the C horizon, and Mg was higher in the Oa horizon.

## 4. Discussion

### 4.1. Comparison of sequential extracts of minerals and soil parent material with mineral compositions

To determine which minerals were dissolved during each step in the extraction procedure, the chemical composition of the extracts of the impure mineral separates were plotted on ternary diagrams with the apices Ca, Mg, and K + Na (Fig. 4), along with the compositions of the individual minerals previously determined by electron microprobe analysis (Nezat et al., 2004). The 1 M $NH_4Cl$ extracts were not plotted because they make up a very small fraction of the total of each element extracted (<0.1%) and they represent an exchangeable pool not associated with the soil mineral pools.

Apatite is the only mineral dissolved in abundance in the 1 M $HNO_3$ (at 20 °C) extracts of the silicate mineral separates and bulk glacial till (Fig. 1). This extract of plagioclase, alkali feldspar, muscovite and the glacial till plots near the apatite composition on the ternary diagrams (Fig. 4), and has P/Ca, Sr/Ca and Na/Ca ratios similar to those of the apatite separate (Table 2). This reflects the selective dissolution of apatite inclusions that occurred

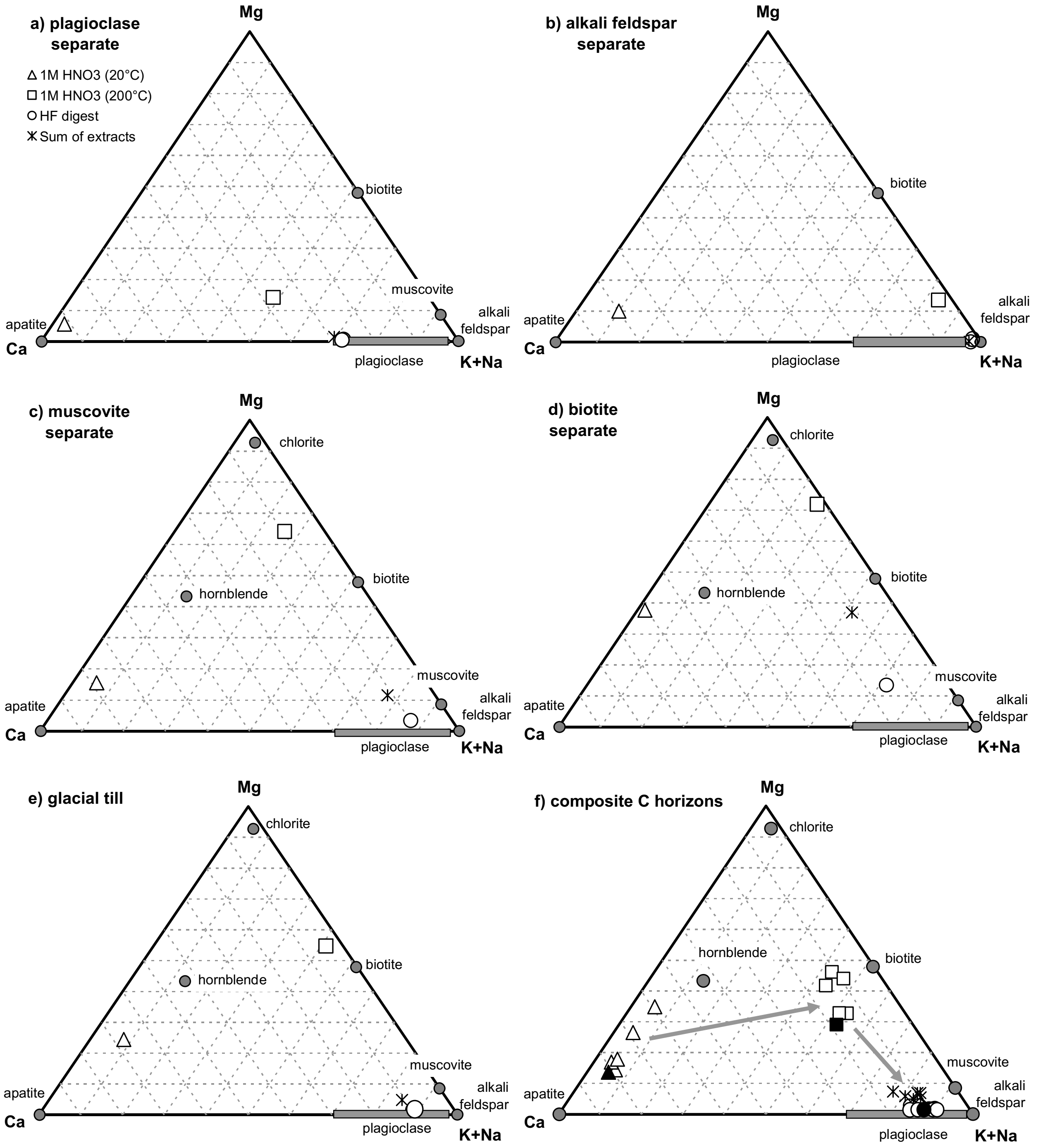

Fig. 4. Ternary diagram comparing chemical composition of sequential extracts of mineral separates, glacial till (from which the minerals were separated), and C horizons to composition of individual minerals. The gray symbols represent the composition of individual mineral as determined from microprobe analysis; the rectangle indicates the range of plagioclase composition in the HBEF soils (data from Nezat et al., 2004). Extracts of the apatite separate are not plotted but would plot on the Ca apex (Table 2). (a) Plagioclase separate. (b) Alkali feldspar separate. (c) Muscovite separate. (d) Biotite separate. (e) Glacial till from which the minerals were separated. (f) C horizon composite soils representing six regions in Watershed 1 at the Hubbard Brook Experimental Forest. The black symbols represent extracts of the C horizon soil that are plotted in Fig. 3. Gray arrows indicate the sequence of extracts from weakest to strongest.

in each of these silicate minerals and were in contact with the extraction solutions (Taylor et al., 2000a). Because the minerals were crushed prior to separation, apatite inclusions that were previously armored by host minerals were exposed. The 1 M $HNO_3$ (at 20 °C) extract of the biotite separate plots between the compositions of apatite and hornblende (an 11% impurity in the biotite separate, Table 1), indicating that some hornblende was dissolved along with apatite in this extract (Table 2).

The composition of the 1 M $HNO_3$ (at 200 °C) extracts of the silicate mineral separates reflects the preferential dissolution of biotite and chlorite (and the apatite inclusions that commonly occur within them) compared to plagioclase, alkali feldspar and muscovite (Fig. 4a–e), as predicted by mineral dissolution kinetics (e.g., Ganor et al., 2005). Although neither biotite nor chlorite was detected in 100 grains analyzed from the alkali feldspar mineral separate by SEM-EDS (Table 1), the composition of this extract suggests that one or both of these minerals is present as an impurity, as is the case for the plagioclase separate, or as inclusions in the alkali feldspar.

The HF solution compositions of each mineral separate (except biotite) plot close to the compositions for the sum of the extracts (Fig. 4) as one would expect, because most of the Ca, Mg, K and Na – the four elements plotted on the ternary diagram – was released in the HF solution (Fig. 1). The HF digest of the biotite separate is an exception because most of the biotite was removed by the previous 1 M $HNO_3$ (at 200 °C) extract. Hence, the composition of the HF solution of biotite plots near the composition of the weathering-resistant minerals that were found as impurities in the biotite "separate" (i.e., plagioclase, alkali feldspar, and muscovite).

To illustrate the utility of the sequential extraction for natural samples, extractions of six composite C horizon samples are compared to the composition of primary minerals (Fig. 4f). These samples were not crushed, and therefore only minerals exposed to soil solutions were extracted by each step. Calcium from apatite as well as some Mg from hornblende and/or chlorite was extracted from the C horizon soils by 1 M $HNO_3$ (at 20 °C). According to the Ca:P ratios in this extract, the source of Ca is apatite (Fig. 5). The scatter of the 6 data points for this extract indicates that the relative proportions of apatite and hornblende/chlorite in the C horizon varied somewhat across the watershed (i.e., W-1 at HBEF).

The composition of the 1 M $HNO_3$ (at 200 °C) extracts of C horizon samples (Fig. 4f) was quite different from the composition of the 1 M $HNO_3$ (at 20 °C) extracts and can be explained by a mixture of apatite (±hornblende), biotite and feldspars. Although most of the apatite was dissolved by the 1 M $HNO_3$ (at 20 °C) extracts, some apatite was not dissolved until the 1 M $HNO_3$ (at 200 °C) step when biotite was dissolved. Biotite can contain numerous apatite inclusions and the dissolution of biotite may expose apatite inclusions to dissolution. The occurrence and dissolution of apatite inclusions in biotite is also supported by the Ca:P ratios of the 1 M $HNO_3$ (at 20 and 200 °C) of the biotite separate (1.9, and 1.7, respectively).

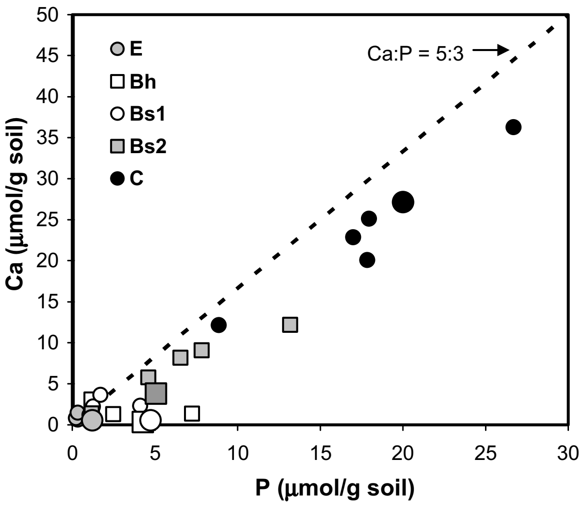

Fig. 5. Calcium versus P extracted from HBEF mineral soil horizons using 1 M $HNO_3$ at 20 °C. These data represent 6 composite soil profiles from HBEF. The variability in chemical composition of the soil horizons is due to differences in vegetation and rates of soil development across the watershed (Nezat et al., 2004). The dashed line represents the Ca:P ratio of apatite (5:3). The enlarged symbols represent the composite soil profile plotted in Fig. 3.

The compositions of the HF solutions of C horizon samples were dominated by K + Na and had a composition similar to that of plagioclase, K feldspar, and muscovite (Fig. 4f). Because plagioclase, alkali feldspar and quartz are the dominant minerals in Hubbard Brook soils (Nezat et al., 2004), the sum of the digests had a composition similar to that of the HF digests, but was shifted slightly toward the composition of the weaker acid extracts.

### 4.2. Isolation of apatite dissolution

Dilute $HNO_3$ concentrations of 0.01 M and 0.1 M were evaluated as potential reagents for the dissolution of apatite from soil parent material, because it was sought to minimize the accompanying dissolution of silicate minerals. However, these solutions were too dilute to dissolve apatite congruently. Thus, a 1 M $HNO_3$ solution was required for apatite extraction. In the 0.01 M $HNO_3$ (Table 3,

Fig. 2), the high ratios of $^{87}Sr/^{86}Sr$ and (Fe + K + Na)/(Ca + Na), and the low Ca/Sr ratio of the minor amount of dissolution product suggest that some biotite dissolution occurred (Erel et al., 2004; Taylor et al., 2000b).

The 0.1 M $HNO_3$ extracts dissolved large amounts of Ca and P (Table 3, Fig. 2), but the Ca:P ratios were considerably higher (~12:3) than the 5:3 ratio of apatite. However, the Ca/Sr and $^{87}Sr/^{86}Sr$ ratios of the 0.1 M extracts were similar to that of the apatite separate (Fig. 2b), confirming that the Ca was derived from apatite. The deficit of P in the 0.1 M extract is probably due to the adsorption of P onto Fe and Al oxides (Dreibus and Haubold, 2004). The Fe content of the 0.1 M extracts is quite low, indicating that Fe oxides were not dissolved under these conditions. Silicate minerals were also not dissolved significantly at this molarity (Table 3).

The 1 M $HNO_3$ extract removed the highest concentrations of Ca and P, had a Ca:P ratio identical to that of apatite (5:3), and had Ca/Sr and $^{87}Sr/^{86}Sr$ ratios similar to that of the apatite separate (Fig. 2b). Relatively high concentrations of K, Mg, Fe and Ti suggest that biotite is also partially dissolved at this molarity (Table 3, Fig. 2c and d). The 1 M $HNO_3$ dissolved ~40 times more Fe than the 0.1 M solution (Table 3). Thus, the 1 M $HNO_3$ solution probably dissolved Fe oxides, which allowed P to remain in solution (Fig. 2c). It is concluded that, to dissolve apatite and keep both Ca and P in solution in an extract, at least a 1 M $HNO_3$ acid strength is necessary.

It was found that temperature had a measurable effect on the extraction of K, Mg, Fe and Ti by 1 M $HNO_3$ (Table 3, Fig. 2), suggesting a minor enhancement of biotite dissolution at higher temperature. Similarly, Bullen and Bailey (2005) found that a 1 M $HNO_3$ extract of similar soils performed at a range of temperatures (0–30 °C) yielded higher K and Mg concentrations and $^{87}Sr/^{86}Sr$ ratios at higher temperatures, which they attributed to enhanced biotite dissolution.

Observing the increased dissolution of biotite with temperature, Bullen and Bailey (2005) used the linear relationship between $^{87}Sr/^{86}Sr$ and K/Sr ratios of soil extracts at different temperatures to estimate the $^{87}Sr/^{86}Sr$ value of non-K-bearing minerals (e.g., apatite and plagioclase). Because the present authors analyzed the $^{87}Sr/^{86}Sr$ ratio of pure apatite separated from the HBEF soils, this assumption can be tested by comparing the measured value of apatite to that predicted by the linear relationship of extracts of HBEF soil parent material at different temperatures and molarities (Fig. 6). The measured $^{87}Sr/^{86}Sr$ of apatite (0.7153) falls within the predicted range (0.7137–0.7217; 95% confidence interval) indicating that Bullen and Bailey's assumption is valid for estimating the $^{87}Sr/^{86}Sr$ ratio of the "K-free component" of soil parent materials.

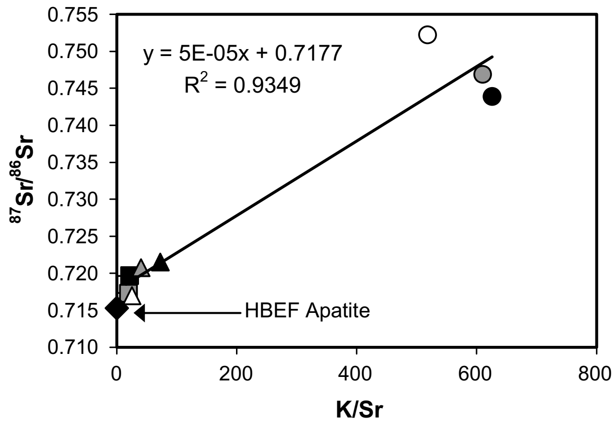

Fig. 6. $^{87}Sr/^{86}Sr$ versus K/Sr ratios of C horizon soil extracted by 1 M $HNO_3$ solution at 0, 10 and 20 °C. As in Fig. 2, the extracts at 0, 10 and 20 °C are represented by open, gray and black symbols, respectively.

It is suggested that a 1 M $HNO_3$ extract of soil is optimal for assessing the amount of apatite that is in contact with soil solutions and thus potentially available to plants by mineral weathering. About 80% of the P in the C horizons of soils was dissolved by these extracts (Fig. 3). The remaining ~20% of P was probably derived from the more resistant (Williams et al., 1980) and less abundant phosphate mineral monazite [(Ce,La,Y,Th)$PO_4$] and from apatite that is entirely included within silicate minerals and thus shielded from the 1 M $HNO_3$ (at 20 °C) solution until the host minerals were dissolved in later steps of the extraction.

Although most of the apatite in soil was dissolved in the 1 M $HNO_3$ at 20 °C, only ~40% of the apatite mineral separate dissolved during this step; the remaining apatite was released by the 1 M $HNO_3$ extracted at 200 °C. Results from the geochemical modeling program, Solmin88, indicate that the 1 M $HNO_3$ extract at 20 °C became saturated with respect to apatite (saturation was reached at ~90 mmol apatite/L solution). Due to the small amount of apatite in soil, the 1 M $HNO_3$ extract of soil did not become saturated with respect to apatite (~0.5 mmol apatite/L solution). Thus, apatite in natural abundance in soil is expected to dissolve completely during this step.

In the case of the plagioclase and alkali feldspar mineral separates, the HF solution also extracted some P, but in amounts much less than predicted by the Ca:P of ratio of apatite, due to Ca also being released from feldspar (Fig. 4). The source of P is predominantly apatite inclusions as in the case of the C horizon samples, as discussed above. The lack of P in the HF digest of biotite and muscovite results indicate that apatite inclusions in the biotite and muscovite were largely dissolved by the 1 M $HNO_3$ extracts at 20 °C and 200 °C.

It should be kept in mind that apatite included in more resistant minerals will not be dissolved until the host minerals are broken down. Thus the sequential extraction described here allows quantification of the amount of apatite in contact with soil solutions, and the amount of apatite armored by silicate minerals with varying degrees of resistance to weathering. To quantify the total amount of apatite in a soil or rock sample, samples should be finely powdered before extraction to fully expose apatite inclusions to the 1 M $HNO_3$ extract (at 20 °C).

### *4.3. Interpreting extracts of soil profiles*

Interpreting the sequential extraction of soil profiles can be complicated because soils contain exchangeable cations, labile and refractory organic matter, and secondary minerals such as Fe and Al oxides, in addition to primary minerals. Elemental concentrations for each extract of each horizon for one representative composite soil profile are shown in Fig. 4, and a few illustrative chemical parameters for each soil horizon from all 6 composite soil profiles investigated are plotted on Figs. 5 and 6. Previous observations were used to help interpret the change in chemical composition of extracts with depth. From an earlier study, it is known that chemical weathering progressively decreases with depth in HBEF soils (Nezat et al., 2004) such that primary minerals are less weathered at depth. For example, earlier studies (Beck and Elsenbeer, 1999; Blum et al., 2002) have documented the presence of apatite in deeper soils but the absence of apatite in upper horizons due to weathering. In addition, it was assumed that (1) the C horizon represents the parent material of the overlying, weathered soils, and (2) minimal weathering has occurred in the C horizon.

The Ca and P contents of the 1 M $HNO_3$ (at 20 °C) extracts of soil horizons indicate that apatite is present only in the deeper soil horizons at HBEF (Figs. 3a,f and 5). In the experiments on mineral separates, it was verified that 1 M $HNO_3$ (at 20 °C) dissolved apatite congruently (Fig. 1a). The Bs2 and C horizons have the highest concentrations of Ca and P in the 1 M $HNO_3$ (at 20 °C) extracts and these elements are released in the apatite Ca:P ratio of 5:3 (Fig. 5). Above the Bs2 horizon, the lack of correlation between Ca and P indicates that these elements reside in different pools (Fig. 5).

As soils develop, primary apatite is weathered from the soil. After release by weathering, Ca is taken up by vegetation, held on the exchange complex, or dissolved in groundwater and lost from the ecosystem. Due to its relative mobility following mineral dissolution, Ca in the 1 M $HNO_3$ (at 20 °C) extracts of the upper horizons has a lower concentration than deeper in the soil where less apatite weathering has occurred. In contrast, P is comparatively immobile in HBEF soils (Wood et al., 1984), and after being released by weathering of apatite is retained in the soil complexed with organic matter and secondary minerals (Cross and Schlesinger, 1995; Johnson et al., 2003; Smeck, 1985; Walker and Syers, 1976), resulting in a relatively constant P concentration above the C horizon. In the organic horizon (Oa), some P is extracted by 1 M $HNO_3$ (at 20 °C), but little Al or Fe, suggesting that the P at this depth is associated with relatively labile organic matter. In the B horizon, elevated concentrations of P accompanied by Al and Fe in the 1 M $HNO_3$ (at 20 °C) extract suggest that P is associated with secondary Al and Fe oxides.

Large amounts of P were also removed by the 1 M $HNO_3$ extract (at 200°C) in the organic and B horizons. Phosphorus in these horizons is correlated with soil organic matter content, measured as loss on ignition at 550 °C (Fig. 7), which suggests that it is associated with more refractory organic matter.

Magnesium concentrations in the 1 M $HNO_3$ extract (at 20 °C) are highest in the B and C horizons indicating the weathering of Mg-bearing minerals in the upper soil profile (Fig. 3). Common Mg-bearing minerals in the HBEF soils are biotite, chlorite and hornblende. The high Mg and Fe concentrations and low K:Mg ratio (0.2–0.4) of this extract suggest that the source of Mg is chlorite or altered biotite (hydrobiotite/vermiculite), rather than biotite (K:Mg ∼ 1; Nezat et al., 2004). The low Na concentration suggests that hornblende is not a major source of Mg in this extract (Fig. 3).

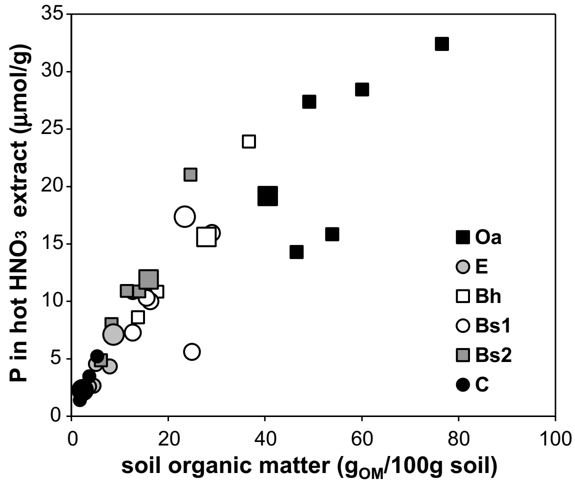

Fig. 7. Phosphorus extracted from HBEF soil horizons by 1 M $HNO_3$ at 200 °C plotted as a function of soil organic matter (measured by loss on ignition; data from Nezat et al., 2004). These data represent six composite soil profiles from HBEF. The enlarged symbols represent horizons from the composite soil profile plotted in Fig. 3.

Most of the Mg-bearing minerals are dissolved by 1 M $HNO_3$ extract (at 200 °C).

Based on comparison with the composition of sequential extractions of the mineral separates, it is concluded that the HF/HCl/$HNO_3$ solution digests mainly plagioclase and alkali feldspar (Fig. 1d–e), which are the dominant minerals in HBEF soil parent materials (in addition to quartz). Assuming that the C horizon represents the initial composition of the upper soil horizons, the decrease in Ca, Na and K towards the soil surface represents the depletion of alkali and plagioclase feldspars by mineral weathering. One limitation of this extraction method is that it does not monitor Si from quartz or feldspar dissolution because Si is lost during the HF digestion and cannot be quantified. Quartz, a major component of granitic rocks, may be a significant source of Si, a biologically important element (Derry et al., 2005). Quartz may also contain inclusions of apatite or silicate minerals. Because these inclusions will dissolve during the HF digest as its host dissolves, inclusions can be quantified by this extraction procedure.

### *4.4. Application to other soil and rock types*

The sequential extraction method described in this study is appropriate for application to igneous and silicate-dominated metamorphic rocks. In the current study, the sequential extraction method was performed on relatively young soils (~14 ka) developed on silicate crystalline rock soil parent materials in a temperate climate. In another study (Nezat, unpublished), this sequential extraction technique was tested on C horizon soils developed on a variety of igneous, metamorphic and sedimentary soil parent materials of varying age from across the northeastern USA. The 1 M $HNO_3$ (at 20 °C) extracts of nearly all soils developed on crystalline silicate rocks (and some clastic non-carbonate sedimentary rocks) exhibited a Ca:P ratio similar to that of apatite, the presence of which was confirmed by mineralogical analysis. In soils developed on sedimentary carbonate rocks, large amounts of Ca and Mg were released by the 1 M $HNO_3$ (at 20 °C) extract indicating the dissolution of carbonate minerals. The release of Ca from carbonate is accompanied by small amounts of P (and Ca:P $\gg$ 5:3) suggesting that the dominant source of Ca in these sedimentary rocks is carbonate minerals but that apatite, most likely as carbonate fluorapatite, is also present in these soils.

## 5. Conclusions

A sequential extraction method was developed and tested to determine the amount of apatite in contact with soil solutions and to quantify its presence as inclusions in more resistant silicate minerals. Applying this method to mineral separates indicated that 1 M $HNO_3$ (at 20 °C) dissolved mainly apatite; 1 M $HNO_3$ (at 200 °C) dissolved mainly biotite and chlorite; and a solution of concentrated HF, HCl and $HNO_3$ (at 200 °C) dissolved muscovite, alkali feldspar and plagioclase feldspar. It was demonstrated that apatite extraction at a 1:10 sample mass:solution ratio could not be carried out with an acid strength of <1 M $HNO_3$ because this molarity is required to assure solubilization of Fe and Al oxides that would otherwise adsorb P.

The sequential extraction method can be applied to soil profiles to provide information about the amount and distribution of pools of mineral-derived nutrients in soils. For example, the amount of apatite available to weathering solutions can be quantified by the amount of Ca and P extracted by 1 M $HNO_3$ (at 20 °C), whereas the Ca and Na concentration of the sum of the extracts can be used to indicate the plagioclase content, because plagioclase is the dominant Ca and Na-bearing mineral. Bulk P concentrations of soils cannot be used to determine the presence of apatite because P is also associated with organic matter and Fe and Al oxides. Hence, sequential extractions can indicate more accurately than bulk soil composition the amount of nutrients held in specific minerals and the potential for these nutrients to be released by weathering.

According to the results of the sequential extraction method, most of the apatite (70%) in the HBEF soil parent material is located along grain boundaries or mineral fractures and is thus available to weathering solutions. The remaining 30% of apatite in HBEF soil parent material is armored by weathering-resistant minerals and appears to be evenly distributed between biotite and feldspars. In HBEF soil profiles, virtually all of the apatite in contact with soil solutions has been weathered from the E and upper B horizons. The 30% of apatite that is armored in silicate minerals remains in the upper soil horizons because it is not in contact with soil solutions. Although some micas and feldspars have been weathered in the upper soil horizons, a large proportion of these minerals remain and thus the release of P by weathering from upper soil horizons is controlled by the kinetics of silicate mineral dissolution, rather than the much faster kinetics of apatite dissolution.

## Acknowledgement

The authors wish to thank T. Siccama, C. Johnson and M. Arthur for insightful discussions that contributed to the development of this extraction procedure. Comments from Gabriel Filippelli and two anonymous reviewers helped to improve this manuscript. This study was funded by grants from the National Science Foundation, the USDA Forest Service, and the University of Michigan. This is a contribution of the Hubbard Brook Ecosystem Study. The Hubbard Brook Experimental Forest is administered by the USDA Forest Service, Northern Research Station, Newton Square, PA, USA.

## References

Aubert, D., Probst, A., Stille, P., 2004. Distribution and origin of major and trace elements (particularly REE, U and Th) into labile and residual phases in an acid soil profile (Vosges Mountains, France). Appl. Geochem. 19, 899–916.

Aubert, D., Stille, P., Probst, A., 2001. REE fractionation during granite weathering and removal by waters and suspended loads: Sr and Nd isotopic evidence. Geochim. Cosmochim. Acta 65, 387–406.

Barton, C.C., Camerlo, R.H., Bailey, S.W., 1997. Bedrock Geologic Map of Hubbard Brook Experimental Forest, Miscellaneous Investigation, Series Map I-2562. U.S. Department of Interior, U.S. Geological Survey.

Beck, M.A., Elsenbeer, H., 1999. Biogeochemical cycles of soil phosphorous in southern Alpine spodosols. Geoderma 91, 249–260.

Blum, J.D., Klaue, A., Nezat, C.A., Driscoll, C.T., Johnson, C.E., Siccama, T.G., Eagar, C., Fahey, T.J., Likens, G.E., 2002. Mycorrhizal weathering of apatite as an important calcium source in base-poor forest ecosystems. Nature 417, 729–731.

Bormann, F.H., Likens, G.E., 1979. Pattern and Process in a Forested Ecosystem. Springer-Verlag, New York.

Bullen, T.D., Bailey, S.W., 2005. Identifying calcium sources at an acid deposition-impacted spruce forest: a strontium isotope, alkaline earth element multi-tracer approach. Biogeochem. 74, 63–99.

Chapin III, F.S., Walker, L.R., Fastie, C.L., Sharman, L.C., 1994. Mechanisms of primary succession following deglaciation at Glacier Bay, Alaska. Ecol. Monogr. 64, 149–175.

Crews, T.E., Kitayama, K., Fownes, J.H., Riley, R.H., Herbert, D.A., Mueller-Dombois, D., Vitousek, P.M., 1995. Changes in soil phosphorous fractions and ecosystem dynamics across a long chronosequence in Hawaii. Ecology 76, 1407–1424.

Cross, A.F., Schlesinger, W.H., 1995. A literature review and evaluation of the Hedley fractionation: applications to the biogeochemical cycle of soil phosphorus in natural ecosystems. Geoderma 64, 197–214.

Davis, M.B., Ford, M.S., Moeller, R.E., 1985. Paleolimnology. In: Likens, G.E. (Ed.), An Ecosystem Approach to Aquatic Ecology: Mirror Lake and its Environment. Springer-Verlag, New York, pp. 345–429.

Derry, L.A., Kurtz, A.C., Ziegler, K., Chadwick, O.A., 2005. Biological control of terrestrial silica cycling and export fluxes to watersheds. Nature 433, 728–731.

Dreibus, G., Haubold, R., 2004. Phosphorous sorption by terrestrial basalt and granite and implications for the martian crust. Icarus 167, 166–169.

Erel, Y., Blum, J.D., Roueff, E., Ganor, J., 2004. Lead and strontium isotopes as monitors of experimental granitoid mineral dissolution. Geochim. Cosmochim. Acta 68, 4649–4663.

Ganor, J., Roueff, E., Erel, Y., Blum, J.D., 2005. The dissolution kinetics of a granite and its minerals–Implications for comparison between laboratory and field dissolution rates. Geochim. Cosmochim. Acta 69, 607–621.

Guidry, M.W., Mackenzie, F.T., 2003. Experimental study of igneous and sedimentary apatite dissolution: control of pH, distance from equilibrium, and temperature on dissolution rates. Geochim. Cosmochim. Acta 67, 2949–2963.

Hamburg, S.P., Yanai, R.D., Arthur, M.A., Blum, J.D., Siccama, T.G., 2003. Biotic control of calcium cycling in northern hardwood forests: acid rain and aging forests. Ecosystems 6, 399–406.

Hannigan, R.E., Sholkovitz, E.R., 2001. The development of middle rare earth element enrichments in freshwaters: weathering of phosphate minerals. Chem. Geol. 175, 495–508.

Hedley, M.J., Stewart, J.W.B., Chauhan, B.S., 1982. Changes in inorganic and organic soil phosphorus fractions induced by cultivation practices and by laboratory incubations. Soil Sci. Soc. Am. J. 46, 970–976.

Johnson, A.H., Frizano, J., Vann, D.R., 2003. Biogeochemical implications of labile phosphorous in forest soils determined by the Hedley fractionation procedure. Oecologia 135, 487–499.

Johnson, C.E., Johnson, A.H., Huntington, T.G., Siccama, T.G., 1991. Whole-tree clear-cutting effects on soil horizons and organic-matter pools. Soil Sci. Soc. Am. J. 55, 497–502.

Köhler, S.J., Harouiya, N., Chaïrat, C., Oelkers, E.H., 2005. Experimental studies of REE fractionation during water–mineral interactions: REE release rates during apatite dissolution from pH 2.8 to 9.2. Chem. Geol. 222, 168–182.

Leleyter, L., Probst, J.-L., 1999. A new sequential extraction procedure for the speciation of particulate trace elements in river sediments. Int. J. Environ. Anal. Chem. 73, 109–128.

Likens, G.E., Bormann, F.H., Pierce, R.S., Eaton, J.S., Johnson, N.M., 1977. Biogeochemistry of a Forested Ecosystem. Springer-Verlag, New York.

Newman, E.I., 1995. Phosphorus inputs to terrestrial ecosystems. J. Ecol. 83, 713–726.

Nezat, C.A., Blum, J.D., Klaue, A., Johnson, C.E., 2004. Influence of landscape position and vegetation on long-term weathering rates at the Hubbard Brook Experimental Forest, New Hampshire, USA. Geochim. Cosmochim. Acta 68, 3065–3078.

Oliva, P., Dupré, B., Martin, F., Viers, J., 2004. The role of trace minerals in chemical weathering in a high-elevation granitic watershed (Estibére, France): Chemical and mineralogic evidence. Geochim. Cosmochim. Acta 68, 2223–2244.

Reiners, P.W., Thomson, S.N., McPhillips, D., Donelick, R.A., Roering, J.J., 2007. Wildfire thermochronology and the fate and transport of apatite in hillslope and fluvial environments. J. Geophys. Res. – Earth Surface.

Ruttenberg, K.C., 1992. Development of a sequential extraction method for different forms of phosphorus in marine sediments. Limnol. Oceanog. 37, 1460–1482.

Schlesinger, W.H., Bruijnzeel, L.A., Bush, M.B., Klein, E.M., Mace, K.A., Raikes, J.A., Whittaker, R.J., 1998. The biogeochemistry of phosphorous after the first century of soil development on Rakata Island, Krakatau, Indonesia. Biogeochem. 40, 37–55.

Smeck, N.E., 1985. Phosphorus dynamics in soils and landscapes. Geoderma 36, 185–199.

Stock, G.M., Ehlers, T.A., Farley, K.A., 2006. Where does sediment come from? Quantifying catchment erosion with detrital apatite (U–Th)/He thermochronometry. Geology 34, 725–728.

Tanner, E.V.J., Vitousek, P.M., Cuevas, E., 1998. Experimental investigation of nutrient limitation of forest growth on wet tropical mountains. Ecology 79, 10–22.

Taylor, A.S., Blum, J.D., Lasaga, A.C., 2000a. The dependence of labradorite dissolution and Sr release rates on solution saturation state. Geochim. Cosmochim. Acta 64, 2389–2400.

Taylor, A.S., Blum, J.D., Lasaga, A.C., MacInnis, I.N., 2000b. Kinetics of dissolution and Sr release during biotite and phlogopite weathering. Geochim. Cosmochim. Acta 64, 1191–1208.

Tessler, A., Campbell, P.G.C., Bisson, M., 1979. Sequential extraction procedure for the speciation of particulate trace metals. Anal. Chem. 51, 844–851.

Valsami-Jones, E., Ragnarsdottir, K.V., Putnis, A., Bosbach, D., Kemp, A.J., Cressey, G., 1998. The dissolution of apatite in the presence of aqueous metal cations at pH 2-7. Chem. Geol. 151, 215–233.

Vitousek, P.M., Farrington, H., 1997. Nutrient limitation and soil development: Experimental test of a biogeochemical theory. Biogeochem. 37, 63–75.

Walker, T.W., Syers, J.K., 1976. The fate of phosphorous during pedogenesis. Geoderma 15, 1–19.

Williams, J.D.H., Mayer, T., Nriagu, J.O., 1980. Extractability of phosphorus from phosphate minerals common in soils and sediments. Soil Sci. Soc. Am. J. 44, 462–465.

Wood, T., Bormann, F.H., Voigt, G.K., 1984. Phosphorous cycling in a northern hardwood forest: biological and chemical control. Science 223, 391–393.

Yanai, R.D., Blum, J.D., Hamburg, S.P., Arthur, M.A., Nezat, C.A., Siccama, T.G., 2005. New insights into calcium depletion in northeastern forests. J. For. 103, 14–20.